Domain Structure and Peculiarities of Surface Morphology of $[(CH_3)_2CHNH_3]_4Cd_3Cl_{10}$ Ferroelastoelectrics

V. Kapustianyk[a], Yu. Chornii[a,*], Z. Czapla[b],
Yu. Eliyashevskyy[a], D. Podsiadła[b] and R. Serkiz[a]

[a]*Department of Physics, Ivan Franko National University of Lviv,
Dragomanova Str. 50, 79005 Lviv, Ukraine*
[b]*Institute of Experimental Physics, University of Wrocław,
pl. M. Borna 9, 50-204 Wrocław, Poland*

The paper is devoted to the study of ferroelastoelectric domain structure and peculiarities of nano- and microcrystals growth on the surface of $[(CH_3)_2CHNH_3]_4Cd_3Cl_{10}$ (IPACC) crystals. The domains in the ferroelastoelectric phase lying below 294 K were visualized using an atomic force microscope. It was shown that the surface morphology of IPACC crystals kept for a long time (from one up to twelve months) in open air undergoes considerable changes in comparison with the freshly cleaved samples. Our samples are characterized by the growth of nanocrystals at the first stage and larger microcrystals at the next stages of the sample aging. Other types of elements observed on the surface were nano- or microrods. The model describing the peculiarities of the surface morphology and domain structure modification arising in the process of aging was proposed.

topics: domains, ferroelastoelectric, nanocrystals, phase transitions

1. Introduction

Unusual structural architectures are formed in halogeno-cadmate(II) compounds. Owing to the chemical flexibility of these hybrid organic–inorganic materials (i.e., the flexibility which accommodates different organic counterions as well as inorganic components), it is possible to create different crystal structures in order to optimize their physical properties [1–9]. For example, the $(CH_3)_2CHNH_3)_4Cd_3Cl_{10}$ (IPACC) crystal with a rather unusual arrangement of the metal–halogen complex belongs to this large family of compounds. It exhibits several temperature-dependent phase transitions and the structures of individual phases were studied. Dielectric, dilatometric, X-ray, DSC and optical studies [10–12] showed and confirmed three phase transitions (PTs). This can be presented in the temperatures scheme

$$Cmca \xrightarrow{T_1} Pbca \xrightarrow{T_2} P2_12_12_1 \xrightarrow{T_3} P2_1/b,$$
$$\text{(I)} \qquad \text{(II)} \qquad \text{(III)} \qquad \text{(IV)}$$

where $T_1 = 353$ K, $T_2 = 294$ K and $T_3 = 260$ K.

The phase transition at $T_1 = 353$ K was associated with the distortion of the anionic sublattice and possesses a displacive character, whereas the remaining transformations are dominated by order–disorder phenomena of the cationic sublattice.

In order to reach a deeper understanding of structural transformations at the phase transitions, we have grown IPACC crystals with a partial substitution of Cd^{2+} ions with Cu^{2+} — $[(CH_3)_2CHNH_3]_4Cd_3Cl_{10}$:Cu (furthermore IPACCC). The Cu^{2+} ion with a surrounding complex was considered as a convenient "probe" in this crystal structure due to the characteristic electron transitions, with the energies corresponding to the visible and near infrared regions of spectra. IPACCC crystals were investigated by the methods based on the crystal field spectra and corresponding program packages as well as on vibrational spectroscopy in order to obtain detailed information about the structural changes at the phase transitions [13–16].

According to the obtained data and also on the basis of X-ray diffraction study [10], the anionic complex for both the IPACC and IPACCC crystals was found to possess the same symmetry. This complex consists of three "metal–halogen" octahedra with different orientation of their axes relatively to the main crystallographic directions [13–16]. This information concerning the phase transitions was complemented by the data of differential scanning calorimetry (DSC) studies [10]. It has been found that IPACCC possesses the sequence of phase transitions very similar to those in the initial

IPACC, although the temperatures of these transitions are a little shifted. They were found to occur at 358, 293, and 253 K during cooling. New IPACCC compounds due to doping with Cu^{2+} ions become of special interest for scientists. They are considered as potential magnetic multiferroics like other related compounds with an alkylammonium cation possessing principally new magnetic properties and magnetoelectric coupling due to the presence of transition metal ions in their structure [17–20].

On the other hand, interest in the initial IPACC crystal grew considerably when the ferroelastoelectric domain structure was visualized for the first time in the analogue doped with copper (in the phase III lying below 293 K) using atomic force microscopy (AFM) [21]. Such data are very important since only a few specific examples of high order ferroics of this type are currently known. This is because the ferroelastoelectric domains are hardly detectable [21, 22].

Under such circumstances, it would be interesting to check whether the ferroelastoelectric domain structure is a peculiar feature only of the doped crystals or it would also be visualized in the initial IPACC. Besides, it would be interesting to compare the obtained data with those for the compound doped with copper. Such investigations are important not only for the fundamental science but also for practical applications. Indeed, the regular domain structure observed in the analogue doped with copper [21] is quite suitable for the creation of diffraction gratings. Under such circumstances, a special attention has to be devoted to a sample stability as well as to the processes of aging in open air and their impact on its surface morphology.

2. Experimental

Transparent IPACC crystals were grown at $T = 304$ K from an aqueous solution of $CdCl_2 \cdot 4H_2O$ and $(CH_3)_2NH_2Cl$ salts taken in the stoichiometric ratio with a small excess of HCl. The grown samples are easily cleaved along ac planes.

The morphology of a sample surface was analysed using an AFM Solver P47-PRO in the contact and semicontact modes and a scanning electron microscope REMMA-102-02 (SELMI, Ukraine).

The elemental chemical composition of the samples was examined by SEM using an energy-dispersive X-ray (EDX) analyzer (the acceleration voltage was 10 kV; K- and L-lines were used).

3. Results and discussion

The data of EDX analysis presented in Fig. 1 confirm the chemical composition of the grown IPACC crystals.
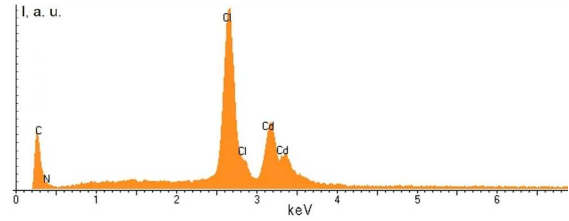
Fig. 1. The EDX analysis data for IPACC crystals averaged over the surface.
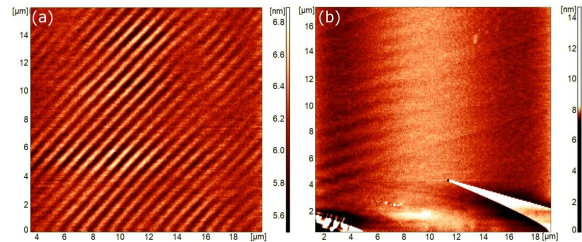
Fig. 2. Domain structure of the freshly cleaved sample of b-cut of IPACC crystal visualized at $T = 280$ K by AFM using contact (a) and semicontact (b) modes.

Investigations of a possible domain structure are of special interest. Normal ferroics such as ferroelastics are easy to identify from optical indicatrices, which are distinct for different domains. In higher order ferroics, distinct twins usually no longer differ in neither spontaneous strains or optical indicatrices and, as a consequence, they are rather difficult to detect [22].

At the equitranslational structural transition $Pbca \rightarrow P2_12_12_1$ (at 294 K) in the investigated crystal, spontaneous piezoelectric tensor components d_{14}, d_{25}, and d_{36} arise [22]. This means that by applying an electric field along the b axis one can obtain mechanical shear deformation in the ac plane and vice versa — the application of the corresponding shear stress will be followed by arising of the polarization along the b direction. The domains would be switched by a simultaneous application of mechanical stress and electric field in appropriate directions.

In order to visualize possible ferroelastoelectric domains, we used the atomic force microscope in the contact and semicontact mode. In these cases, we investigated the freshly cleaved thin samples of b-cuts (see Fig. 2). First of all, the temperature of a sample was stabilized at the constant temperature $T = 280$ K far below the phase transition at $T_2 = 294$ K. In the contact mode, one can observe a regular pattern of the parallel strips with an average thickness of nearly 1 μm that would be considered as domains (see Fig. 2). It is necessary to note that the domain boundaries are also seen in the semicontact mode although the pattern is less distinct. These data show that the contact mode is more convenient for the visualization of the ferroelastoelectric domain pattern.
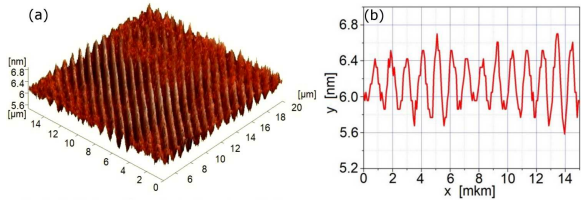
Fig. 3. 3D presentation (a) and profile (b) of the surface presented in Fig. 2a.

In order to draw more convenient information from the AFM data, we prepared a 3D presentation (Fig. 3a) and profile (Fig. 3b) of the sample surface presented in Fig. 2a. As it is clearly seen, the average thickness of the domains is 1 μm, whereas the difference in heights of this regular relief was found to be varied from 0.5 nm up to 1 nm.

A special question needs to be answered: why is it possible to distinct the ferroelastoelectric domains in the contact mode of AFM. One can suggest that the main reason is the shear stress arising when the sample is cleaved. The stress appears in the *ac* plane. Taking into account that the neighboring ferroelastoelectric domains differ by the sign of the component of the piezoelectric effect tensor, they should be distinguished by a sign of the electric polarization. Under such circumstances, the problem of the domains visualization looks very similar to that in the ferroelectrics. The conventional contact mode of AFM has been used for domain studies via investigation of the domain-related surface morphology of ferroelectrics [23].

There are several mechanisms which can provide morphological contrast of ferroelectric domains: (1) topographic steps at domain boundaries due to the structural difference between positive and negative ends of domains; (2) inclination of the cleaved surfaces according to the polarity of domains and the direction of cleavage propagation [23]. The second mechanism looks more sufficient to explain the observed domain pattern in the investigated ferroelastoelectric.

The next stage of our experiments was devoted to the study of the influence of crystal aging on its domain pattern and surface morphology. In the aged sample, we observed in the contact mode a less regular structure with a domain thickness varying from 2 to 3 μm and the difference in heights of this regular relief was found to be varied up to 100 nm (Fig. 4b). The mentioned sample after cleavage was kept at open air atmosphere for a long time — close to one month. One can mention that such samples are characterized by the appearance of peak-like elements with a diameter starting from hundreds of nanometers up to a few micrometers and the heights — from a few tens of nanometers up to 200 nm. Growth of similar nano- and microcrystals was already observed on the surface of other crystals with an alkylammonium cation [24] as well as in the
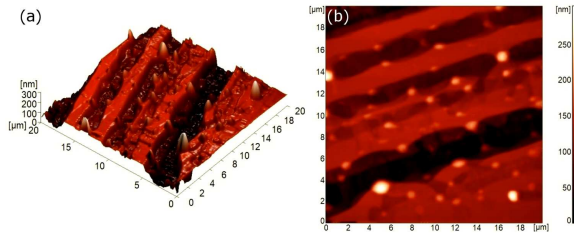
Fig. 4. Domain structure of the aged sample of *b*-cut of IPACC crystal, kept in open air for at least one month, visualized at $T = 293$ K by AFM using contact mode (a) and corresponding 3D presentation (b).
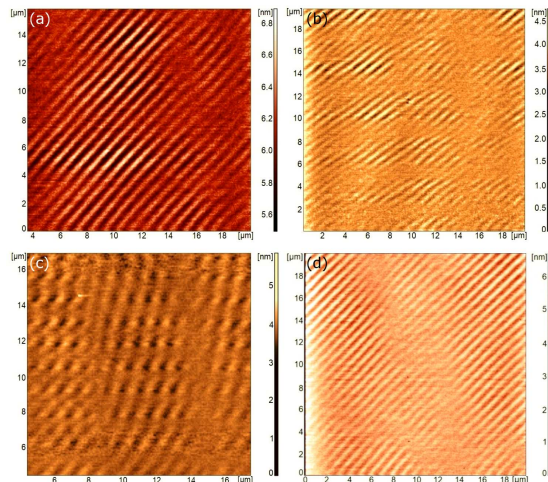
Fig. 5. The evolution of the domain structure under temperature in a freshly cleaved sample of IPACC crystals in the vicinity of the phase transition at $T_2 = 294$ K. The considered temperatures in the regimes of heating are (a) $T = 293$ K, (b) $T = 294$ K, up to (c) $T = 297$ K, and further cooling at (d) $T = 293$ K.

layered compounds like cadmium iodide [25]. The models of the corresponding processes were fairly well described in the mentioned papers.

Comparing the images presented in Figs. 2–4 one can conclude that the character of the domain structure, the domain width as well as the heights of the relief elements depends on a sample, and first of all, on its preceding history.

In order to confirm that quite a regular strip-like pattern observed in a freshly cleaved sample is really connected with a domain structure, we performed its investigations in a contact mode in the temperature region below and above the phase transition point $T_2 = 294$ K (Fig. 5). The domain pattern which is distinct at $T = 280$ K becomes less clear at approaching phase transitions and practically disappears in the high temperature phase II. Nevertheless, during cooling the domains appear again below $T_2 = 294$ K.

During heating, the domain structure did not disappear at the moment of approaching the phase transition point. In some part of the sample it was
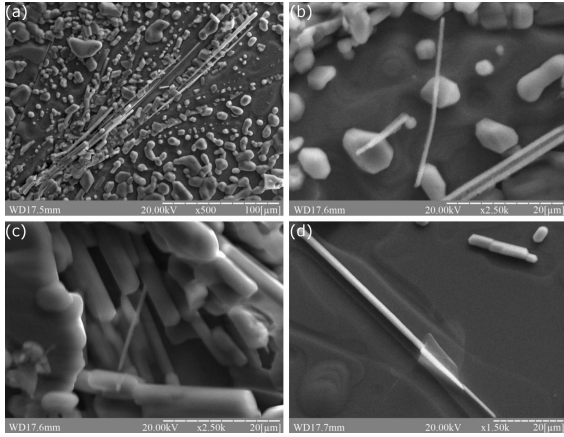
Fig. 6. SEM images of IPACC of various regions of the aged crystal surface presented in different scale (a)–(d).

still observed until the temperatures a little higher than T_2. A similar retardation in restoring the domain structure was observed in the vicinity of this point at cooling. Such a behavior is characteristic of the first order phase transitions. On the other hand, one can suppose that the crystal surface stays periodically corrugated even during a certain time after the disappearance of the domain structure at heating above T_2 due to the remnant deformation of the sample.

It is necessary to note that different freshly cleaved samples of IPACC crystals are characterized by a very similar regular structure with very close sizes of domains. Moreover, the surface of the crystal is modulated with an amplitude close to 1 nm. The neighboring domains should differ by their optical characteristics, first of all, by the refractive indices due to a different sign of the electrooptic effect [23]. Due to this, IPACC crystals could be used as the diffraction grating with a period close to 1 μm.

Let us consider in detail the nano- and microcrystals arising at the single crystal surface of IPACC at the process of aging. The observed phenomenon appeared to be strongly dependent on time. When the sample was kept in open air during 12 months, the mentioned microcrystals became much larger and covered practically the entire surface of the single crystal (see Fig. 6a). It is clear that their sizes vary within the framework from 0.5 to 10 μm. In this case, the scanning electron microscopy looks much more sufficient for the study of the crystal surface morphology. Figure 6b presents the mentioned microcrystals in a more detailed scale. It is interesting to note that their habit looks very similar to that of the bulk single crystal. Another interesting feature of the surface morphology is the appearance of the nanorods at the late stage of aging (Fig. 6c, d). Their diameter varies from 1 to 4 μm and their length reaches few tens of μm.

On the basis of the performed investigations, one can propose the following model of the nano- and microcrystals growth on the surface of the IPACC bulk crystal. At sufficiently high humidity of atmospheric air due to a little hygroscopic nature of the sample, water from the atmosphere is absorbed and condensed on a crystal surface. The crystal is dissolved creating a saturated solution. According to the data concerning a crystal similar in its chemical composition [24], such a process is realized when the reciprocal humidity reaches at least 70%. When the humidity or temperature of the environment decrease, the solution becomes supersaturated and there starts a process of the nanocrystals growth. At the next stages of this process, they grow up to the micrometer sizes. Such a process is realized due to the surface tension, when the water droplet covers a nano- or microcrystal and a surrounding area of a bulk crystal. The dissolution and growth of the nano- or microcrystals alternate one after another [24].

It is interesting to note that according to the data of the EDX analysis, the observed nanorods are characterized by some small content of oxygen atoms. This could testify that the nanorods may contain the crystallization water. Unfortunately, the EDX analysis is not sufficiently sensitive and precise for a quantitative analysis of such elements like oxygen. Therefore, such a conclusion has to be confirmed by independent, more precise methods.

The water condensed from the atmosphere on the crystal surface also causes a specific etching of the sample. One can suppose that the etching rate is different for the neighboring domains, that is, depends on the sign of the corresponding piezoelectric coefficient. Taking into account the mentioned mechanical stress arising at the process of crystal cleavage, one can conclude that these domains also possess a different sign of polarization on the investigated surface. Due to this, the domain structure causes much more pronounced modulation of the aged sample surface in comparison with the freshly cleaved one. Such an effect is already known for the ferroelectrics. Indeed, for the hydrophilic materials, such as TGS and GASH, when exposing a sample to humid atmosphere, one can reveal the ferroelectric domains due to selective surface etching by the water vapor [23].

4. Conclusions

Using the methods of AFM microscopy we confirmed that IPACC crystals are characterized by the ferroelastoelectric domain structure similar to that in the same crystal doped with copper (IPACCC). On the other hand, one can suggest that a considerable difference was observed in both compared crystals. In IPACCC, the regular pattern of the parallel strips with an average thickness of nearly 4 μm was superimposed with the system of thinner strips (nearly 1 μm). The boundaries of the

smaller domains were found to be turned in respect of the boundaries of the larger domains by the angle a little less than 100° [21]. On the basis of the performed investigations of different IPACC samples, one can conclude that the initial crystals possess only one type of domains. It seems that doping with copper would considerably change the parameters of the ferroelastoelectric domain structure.

The surface morphology of IPACC crystals kept for a long time (from one up to twelve months) in open air undergoes considerable changes in comparison with the freshly cleaved samples. The samples are characterized by the growth of nanocrystals at the first stage and larger microcrystals at the next stages of the sample aging. Such a behavior was related to a little hygroscopic nature of IPACC. At the sufficiently high humidity of the environment, the atmospheric water condensed on the bulk crystal surface causes the alternating process of bulk crystal dissolution and nano- or microcrystal growth. By their shape, these nano- or microcrystals look very similar to the bulk crystal habit.

Another type of the elements observed on the surface would be considered as nano- or microrods. According to the qualitative data of the EDX analysis, they would contain oxygen that may be connected with the formation of the crystal hydrate compound.

The water condensed from the atmosphere on the crystal surface also causes a specific etching of the sample with a different rate for the neighboring domains. One can suggest that this process depends on the sign of the corresponding piezoelectric coefficient or the sign of the polarization caused be the shear mechanical stress arising at the process of crystal cleavage.

In order to avoid the mentioned processes connected with the influence of atmospheric water, IPACC samples should be kept at conditions of low humidity.

It is interesting to note that no similar processes of aging were detected in IPACCC crystals doped with copper [21]. Due to this, such materials look more suitable for the mentioned practical applications.

Acknowledgments

References

[1] Ch.E. Costin-Hogan, Ch.L. Chen, E. Hughes, A. Pickett, R. Valencia, N.P. Rath, A.M. Beatty, *Cryst. Eng. Comm.* **10**, 1910 (2008).

[2] A. Thorn, R.D. Willett, B. Twamley, *Cryst. Growth Des.* **5**, 673 (2005).

[3] S. Sveleba, V. Mokryi, I. Polovinko, V. Zhmurko, V. Kapustianik, J. Stankowski, Z. Trybula, W. Kempinski, *Phase Transit.* **46**, 245 (1994).

[4] V.B. Kapustianik, I.I. Polovinko, S.A. Sveleba, O.G. Vlokh, Z.A. Bobrova, V.M. Varikash, *Phys. Status Solidi A* **133**, 45 (1992).

[5] Wei-Qiang Liao, Guang-Quan Mei, Heng-Yun Ye, Ying-Xuan Mei, Yi Zhang, *Inorg. Chem.* **53**, 8913 (2014).

[6] Guang-Quan Mei, Wei-Qiang Liao, *J. Mater. Chem. C* **33**, 8535 (2015).

[7] Y. Lu, Z. Wang, H.-P. Chen, J.-Z. Ge, *Cryst. Eng. Comm.* **19**, 1896 (2017).

[8] Q. Ji, L. Li, S. Deng, X. Cao, L. Chen, *Dalton Trans.* **47**, 5630 (2018).

[9] M.S. Lassoued, A. Lassoued, M.S.M. Abdelbaky, S. Ammar, A. Ben Salah, A. Gadri, S. García-Granda, *J. Mol. Struct.* **1165**, 42 (2018).

[10] A. Gago, A. Waśkowska, Z. Czapla, S. Dacko, *Acta Cryst. B* **67**, 122 (2011).

[11] B. Staśkiewicz, S. Dacko, Z. Czapla, *Curr. Appl. Phys.* **12**, 413 (2012).

[12] J. Przesławski, M. Kos, Z. Czapla, *Thermochim. Acta* **546**, 49 (2012).

[13] V. Kapustianyk, P. Yonak, V. Rudyk, Z. Czapla, D. Podsiadla, Yu. Eliyashevskyy, A. Kozdraś, P. Demchenko, R. Serkiz, *J. Phys. Chem. Solids* **121**, 210 (2018).

[14] V. Kapustianyk, P. Yonak, R. Serkiz, Yu. Chorniy, Z. Czapla, *J. Phys. Stud.* **23**, 3704 (2019).

[15] V. Kapustianyk, Yu. Chornii, Z. Czapla, O. Czupinski, *J. Phys. Stud.* **24**, 3703 (2020).

[16] V. Kapustianyk, Yu. Chornii, V. Rudyk, Z. Czapla, R. Cach, O. Kolomys, B. Tsykaniuk, *Acta Phys. Pol. A* **138**, 488 (2020).

[17] B. Kundys, A. Lappas, M. Viret, V. Kapustianyk, V. Rudyk, S. Semak, Ch. Simon, I. Bakaimi, *Phys. Rev. B* **81**, 224434 (2010).

[18] V. Kapustianyk, V. Rudyk, P. Yonak, B. Kundys, *Phys. Status Solidi B* **252**, 1778 (2015).

[19] Y. Tian, A. Stroppa, Y. Chai, L. Yan, S. Wang, P. Barone, S. Picozzi, Y. Sun, *Sci. Rep.* **4**, 6062 (2014).

[20] V. Kapustianyk, Yu. Eliyashevskyy, Z. Czapla et al., *Sci. Rep.* **7**, 14109 (2017).

[21] V. Kapustianyk, Z. Czapla, V. Rudyk, Yu. Eliyashevskyy, P. Yonak, S. Sveleba, *Ferroelectrics* **540**, 212 (2019).

[22] Yu.A. Iziumov, V.N. Syromyatnikov, *Phase Transitions and Crystal Symmetry*, Kluwer Academic, Dordrecht 1990.

[23] A.K. Tagantsev, L.E. Cross, J. Fousek, *Domains in Ferroic Crystals and Thin Films*, Springer, New York 2010.

[24] N.A. Loboda, V.B. Kapustianyk, Yu.I. Eliyashevskyy, B.Ya. Kulyk, R.Ya. Serkiz, Z. Czapla, R.Ya. Biliak, *J. Phys. Stud.* **22**, 2703 (2018).

[25] I.M. Bolesta, I.N. Rovetskii, Z.M. Yaremko, I.D. Karbovnyk, S.R. Velgosh, M.V. Partyka, N.V. Gloskovskaya, V.M. Lesivtsiv, *Ukr. J. Phys.* **60**, 1143 (2015).